Key Factors Limiting the Open Circuit Voltage of n+pp+ Indium Phosphide Solar Cells

Chandra Goradia and William Thesling
Space Photovoltaic Research Center
Electrical Engineering Department
Cleveland State University
Cleveland, OH

Irving Weinberg
NASA Lewis Research Center
Cleveland OH

Introduction

Solar cells made from gallium arsenide (GaAs), with a room temperature bandgap of $E_g = 1.43$ eV have exhibited the best measured open circuit voltage (V_{oc}) of 1.05 V at 1 AM0, 25C [ref. 1]. The material InP is in many ways similar to GaAs. A simple calculation comparing InP to GaAs then shows that solar cells made from InP, with $E_g = 1.35$ at 300K, should exhibit the best measured V_{oc} of ~950 mV at 1 AM0, 300K. However, to date, the best measured V_{oc} for InP solar cells made by any fabrication method is 899 mV at AM1.5, 25°C [ref. 2], which would translate to 912 mV at 1 AM0, 25°C.

The V_{oc} of an n^+pp^+ InP solar cell is governed by several factors. Of these, some factors, such as the thickness and doping of the emitter and base regions, are easily controlled and can be adjusted to desired values dictated by a good performance-optimizing model. Such factors have not been considered in this investigation. There are other factors which also govern V_{oc}, and their values are not so easily controlled. The primary ones among these are 1) the indirect or Hall-Shockley-Read lifetimes in the various regions of the cell, 2) the low-doping intrinsic carrier concentration n_i of the InP material, 3) the heavy doping factors in the emitter and BSF regions, and 4) the front surface recombination velocity S_F. We have investigated the influence of these latter factors on the V_{oc} of the n^+pp^+ InP solar cell and have used the results to produce a near-optimum design of the n^+pp^+ InP solar cell.

Theoretical Approach

We have developed a fairly comprehensive, one dimensional, closed form solution, computerized model of the shallow homojunction InP space solar cell. This model assumes a cell with three homogeneously doped regions, an n^+ emitter, a p-type base and a p^+ BSF region. Details of the model have been presented elsewhere [ref. 3]. In our earlier near-optimum design of the n^+pp^+ shallow-homojunction InP solar cell using this model [refs. 3,4] no accounting was made of the heavy-doping effects in the

heavily doped emitter and BSF regions. As of this day, to the best of our knowledge, measured heavy doping factors or equivalent bandgap narrowing values as functions of doping for n-type and p-type InP have not been published in the literature, as they have been for GaAs [ref. 5]. This lack of information makes it difficult to take into account heavy doping effects in InP cell modeling. Even so, it is now realized that it is very important to take these into account in order for the modeling to be of much value. Hence, some way must be found to reasonably estimate the heavy doping effects. A prior attempt [ref. 6] at this has been to represent the heavy doping effects, including Fermi-Dirac statistics, by an equivalent effective bandgap narrowing ΔE_g in each heavily doped cell region (emitter, BSF) and to estimate the amount of ΔE_g in these regions by matching the calculated and measured internal spectral response in the short and long wavelength region of the incident light spectrum. We feel that a less roundabout and more accurate method is to lump all the heavy doping effects into an effective intrinsic carrier concentration n_{ie} and to thereby define a heavy doping factor HD in each heavily doped region as, for example in the emitter, by

$$HD_E = \frac{n_{ieE}}{n_{i0}}$$

where n_{ieE} is the the effective value of n_i in the emitter and n_{i0} is the low-doping value of n_i in InP. A similar heavy doping factor HD_{BSF} is defined for the BSF region. The values of HD_E and HD_{BSF} are then estimated by matching the calculated and measured curves of not only the internal spectral response but also the illuminated I-V and log $I_{sc} - V_{oc}$.

The above approach still leaves one major problem. It allows the estimation of HD_E and HD_{BSF}, each for only one value of doping, that of the experimental cell whose measured curves were matched. However, what is needed for general modeling purposes is HD_E and HD_{BSF} as functions of their respective dopings: in other words, curves of HD_E^2 and HD_{BSF}^2 vs. their respective dopings, as are available for GaAs at 300K [ref. 5], as shown in figure 1. In the absence of available measured data on InP, we made the reasonable assumption, as a first approximation, that for both n-type and p-type InP, the nature of the HD^2 versus doping curve is similar to that of GaAs. With this assumption, the curve for InP can be obtained from that of GaAs if one point on the curve could be determined. As stated earlier, this can indeed be done by matching the calculated and measured curves of illuminated I-V, log $I_{sc} - V_{oc}$ and internal spectral response.

Our computer model was designed from the start to correctly take into account heavy doping effects in all three regions of the cell,if necessary, by means of appropriate boundary conditions involving the heavy doping factors in each region. The boundary condition at the emitter-base junction is that of the generalized 'law of the junction', valid at all injection levels, while that at the base-BSF interface is that of the low-injection effective interface recombination velocity S_{pp+} given by

$$S_{pp^+} = \frac{N_{a,base}}{N_{a,BSF}} \cdot \left(\frac{HD_{BSF}}{HD_{base}}\right)^2 \cdot \frac{D_{n,BSF}}{L_{n,BSF}} \cdot \frac{1}{\tanh(\frac{w_{BSF}}{L_{n,BSF}})} \quad [1]$$

where N_a is the doping, HD is the heavy doping factor, as defined earlier (e.g. $HD_{BSF} = n_{ie,BSF}/n_{i0}$), and D, L, w are the minority carrier diffusivity, diffusion length and width of the region, respectively. For a base doping of less than 10^{17} cm^{-3}, $HD_{base} = 1$, and it is seen in equation [1] that the net effect of heavy doping in the BSF region is to increase the effective base-BSF interface recombination velocity S_{pp^+} by a factor of $(HD_{BSF})^2$. As we shall see from the calculated results in the following section, the overall effect of heavy doping in the BSF region is to increase the minority carrier recombination in the base at the base-BSF interface, thereby increasing the dark saturation current in the base and reducing the open circuit voltage of the cell.

As to the task at hand, that of finding HD_E and HD_{BSF} at one doping, we chose to match theoretical and measured curves of illuminated I-V, log I_{sc} – V_{oc} and internal spectral response for a 17.9% efficient n^+pp^+ solar cell labeled Spire 6 [ref. 7], made by the Spire Corporation, for which such measured curves were available. All measurements on this cell were made at the NASA Lewis Research Center in Cleveland, Ohio, and were made available to us by courtesy of Mr. Russell E. Hart.

We obtained excellent matches between the calculated and measured curves of Spire 6 for specific values of $HD_E = 1.4$ for the n-type emitter doping of 1×10^{18} cm^{-3} and $HD_{BSF} = 4.87$ for the p-type BSF doping of 5×10^{18} cm^{-3}. By noting that each of the two HD^2 versus doping curves had to pass through its corresponding specific point indicated above and also that each HD has to become unity at dopings of 10^{17} cm^{-3} and below, we were able to express the general variations of HD_E and HD_{BSF} versus their respective dopings in equation form as:

$$HD^2_{E,n-InP} = 1.92 \cdot [HD^2_{n-GaAs} - 1] + 1 \quad [2]$$

except when HD_{n-GaAs} drops below unity, in which case, for simplicity, we used the approximation

$$HD^2_{E,n-InP} = HD^2_{n-GaAs} \quad [3]$$

Also,

$$HD^2_{BSF,p-InP} = 6.1 \cdot [HD^2_{p-GaAs} - 1] + 1 \quad [4]$$

The +1 on the right-hand side of equations [2] and [4] ensures that HD in InP becomes unity when HD in GaAs becomes unity, at the lower dopings.

The above equations were incorporated into the computer model so that, for any doping concentration in the emitter and BSF, the corresponding heavy doping factor could easily be calculated. This capability to calculate the heavy doping factors HD_E, HD_{BSF} as functions of doping was the only new addition that our computer model required. The computer model was already capable of calculating all other geometrical and material parameters needed to simulate the solar cell, as in the past [refs. 3,4].

Calculated Results and Discussion

In order to see how the V_{oc} varied with each of the individual parameters expected to affect it, we first chose a somewhat modified version of the Spire 6 cell design to serve as a baseline cell. The primary modifications were: a) a reduced grid shadowing from 4.8% of Spire 6 to 4.0% of the baseline design, b) a thinner emitter, from 400Å of Spire 6 to 200Å of the baseline cell, c) a heavier emitter doping, 5×10^{18} cm^{-3} from 1×10^{18} cm^{-3} of Spire 6, d) a thinner base, 2 μm instead of 3 μm, and e) a lighter BSF doping of 2×10^{18} cm^{-3} for the baseline cell instead of 5×10^{18} cm^{-3} for Spire 6. These modifications reflected current practice in cell design and resulted in an improved cell efficiency of 19.23% from the 17.9% of Spire 6. The baseline design also resulted in a somewhat larger V_{oc} of 873 mV from the 868 mV of Spire 6. Table 1 shows all the geometrical and material parameters of the Spire 6 and the baseline solar cells. Note that the numbers in the baseline cell column are for 300 K as opposed to 298 K for Spire 6. This results in a significantly longer radiative lifetime in the base for the baseline cell, since the base radiative lifetime is extremely sensitive to temperature.

In our model, the indirect or Hall Shockley-Read (HSR) lifetime in any cell region is assumed to be inversely proportional to the doping in that region. This assumption is tantamount to the assumption that indirect recombination in InP occurs via a single dominant recombination level whose density is proportional to doping density. Thus, in any cell region,

$$\tau_{HSR} = \frac{\Gamma_{HSR}}{N} \qquad [5]$$

where Γ_{HSR} is the constant of proportionality between τ_{HSR} and the reciprocal of the doping concentration N. Only two different values of Γ_{HSR} are needed, one for n-type and one for p-type InP. These were obtained from our matching the calculated and measured curves for Spire 6, as were the values of HD_E, HD_{BSF} and S_F. For the baseline value of n_i, we chose the prevalent value of $n_i(300\ K) = 1.2 \times 10^7 cm^{-3}$, which may be on the high side according to current thinking [ref. 2].

Thus, knowing the baseline values of HD_E, HD_{BSF}, $\Gamma_{HSR,p}$, $\Gamma_{HSR,n}$, S_F and n_i, all except n_i being derived from the Spire 6 match, we could calculate the complete performance of the baseline cell at 300 K. The second column of Table 1 gives the

geometrical, material and performance parameters of the baseline cell. Note that the baseline cell has a thinner, more heavily doped emitter, a thinner base and a less heavily doped BSF layer than the Spire 6 cell.

Next, we made a large number of parametric variation runs of our computer model simulating the baseline cell, varying one parameter at a time from among HD_E, HD_{BSF}, $\Gamma_{HSR,p}$ and $\Gamma_{HSR,n}$ (in the form of relative HSR or indirect lifetime τ_i/τ_{i0} in the n-type emitter and p-type base and BSF regions), the low-doping intrinsic carrier concentration n_{i0} and finally the front surface recombination velocity S_F. It should be noted that in our model, S_F is the area-weighted average effective surface recombination velocity over both the part of the front surface which is not in actual physical contact with the front grid metallization and the part which is in such contact [ref. 3].

The results of the parameter variation runs are shown in Figs. 2,3,4 and 5, which show, respectively the variation of V_{oc} versus 1) the HSR relative lifetime τ_i/τ_{i0} in the emitter, base and BSF, 2) the low-doping intrinsic carrier concentration n_{i0}, 3) the BSF heavy doping factor HD_{BSF} and 4) the effective front surface recombination velocity S_F.

We now discuss each of these figures in turn. In Fig. 2, we see that if, by using better material and device processing, we can make the indirect or HSR lifetimes in all regions of the cell to be ten times longer than their current-technology values in Spire 6, then V_{oc} can be improved by slightly over 10 mV, which, while not being a very large gain in V_{oc} still is a significant gain. Fig. 2 also shows that V_{oc} begins to level off as the HSR lifetime is made even longer. This is because when the HSR lifetime becomes very long, the overall lifetime is controlled by the radiative lifetime which, for a given doping and temperature, is an inherent property of the material InP and is independent of the quality of the starting material or of the device processing parameters. Thus, it appears from Fig. 2 that by making the HSR lifetime in each region indefinitely long by using the highest quality starting material and using the cleanest possible device processing, the most to be gained in V_{oc} is about 15 mV or so.

Next considering Fig. 3, we see the variation in V_{oc} as the 300 K, low-doping intrinsic carrier concentration n_{i0} decreases from $1.2\times10^7 cm^{-3}$ to a hypothetical value of 5×10^6 cm^{-3}, to show the nature and extent of variation of V_{oc} with n_{i0}. If n_{i0} were somehow halved from its presently used value of 1.2×10^7 cm^{-3} to 6×10^6 cm^{-3}, then Fig. 3 shows that V_{oc} would increase by ~25 mV. The values of n_{i0} and V_{oc} indicated by the two arrows in Fig. 3 are as follows. The one corresponding to n_{i0} = 1.2×10^7 cm^{-3} represents the prevalent value of n_i based on both the density of states functions N_c, N_v, and the bandgap E_g corresponding to InP. The other point is the value of n_{i0} that would be obtained by using the density of states values of GaAs but the bandgap of InP–in other words, the value of n_i that InP would have if its N_cN_v product were the same as that for GaAs. The difference in V_{oc} between the

two points is about 18 mV, and it indicates that, in comparison with GaAs, InP has an 18 mV V_{oc} disadvantage merely because its N_cN_v product is too large compared to that of GaAs.

There is some uncertainty about the value of n_i in InP. Yahia and Coutts have done an extensive investigation of this problem, and believe that n_i in InP at 300 K should be around 8 to 9×10^6 cm^{-3} [ref. 8]. If this is true, then the expected maximum V_{oc} of InP would be higher by about 10 mV.

In Fig. 4, we show the calculated variation of V_{oc} for the baseline InP cell with the BSF heavy doping factor $HD_{BSF} = n_{ie,BSF}/n_{i0}$ The point corresponding to the heavy doping factor calculated using equation (4) is indicated by the arrow. It is seen that the lower the heavy doping factor, the higher the V_{oc}.

If the qualitative behavior of heavy doping factor versus doping in p-type and n-type InP is indeed similar to that for GaAs, as we have assumed, then it would appear at first sight that it would be advantageous to have an n-based cell with n^+ BSF. However, only detailed calculations would show whether that would be the case or not, for the following reasons: First, in a p^+nn^+ InP cell, the p^+ emitter would have to be relatively thick in order for the low hole mobility in it to not cause an excessively large emitter sheet resistance component of series resistance. With a thicker emitter, a significant portion of the total cell photocurrent would now come from the emitter, as would the dark saturation current. In that case, any gain due to a low (lower than one) HD_{BSF} could be more than counteracted by the high HD_E in the p^+ emitter. We are in the process of doing such detailed calculations for the p^+nn^+ cell.

Finally, Fig. 5 shows the variation of V_{oc} versus the effective front surface recombination velocity S_F. Here, it is seen that over its entire range of values from $S_F \ll D_{pE}/L_{pE}$, the diffusion velocity of minority carriers in the emitter, to $S_F \gg D_{pE}/L_{pE}$, V_{oc} degrades by only about 3 mV. The reason why V_{oc} is relatively insensitive to S_F is that in any relatively well-designed InP solar cell, as in the baseline cell, the V_{oc} is controlled primarily by the dark saturation current J_0 in the base, which is several times (~10 or more) larger than the J_0 from the emitter. Thus, the S_F variation, which may affect $J_{0,emitter}$ by a factor of a few, does not affect the overall J_0, and therefore V_{oc}, significantly. It is to be noted, however, that S_F has a significant effect on the short circuit current J_{sc} and on the efficiency; therefore, it is most desirable to reduce S_F to a very low value ($S_F \ll D_{pE}/L_{pE}$) by means of front surface passivation or the use of an appropriate higher bandgap window layer.

Near–Optimum Cell Design

Having investigated the individual variation of V_{oc} with each of the parameters $\Gamma_{HSR,n}$ and $\Gamma_{HSR,p}$, n_{i0}, HD_{BSF} and S_F and some other variations (V_{oc} vs. base thickness, base doping, emitter thickness, emitter doping and HD_E) not shown here,

we next proceeded to design a near-optimum InP n^+pp^+ solar cell for 1 AM0, 300 K operation with a view to maximizing its efficiency (not V_{oc})

Our approach to the near-optimum design was to ignore limitations imposed by current technology on such parameters as $\Gamma_{HSR,p}$, $\Gamma_{HSR,n}$ and S_F. With improved technology, in the near future, $\Gamma_{HSR,p}$ and $\Gamma_{HSR,n}$ could realistically be about ten times the values obtained in the Spire 6 match, while S_F could very likely be $\sim 10^4$ cm/s or less. Thus we have used values for $\Gamma_{HSR,p}$ and $\Gamma_{HSR,n}$ that are ten times the values obtained in the Spire 6 match and used in the baseline cell. This is tantamount to assuming that in the near future, material and processing quality is likely to improve to the extent that at moderate and high dopings, the overall lifetime in InP will be limited by the radiative lifetime. We have also used $S_F = 10^4$ cm/s, again assuming that the significant amount of research on surface passivation and searching for an appropriate window material will result, in the near future, in an effective front SRV of $S_F = 10^4$ cm/s or less. As to the technology-independent parameters, such as HD_E, HD_{BSF} and n_{i0} we have used the same values as used earlier, namely, HD_E and HD_{BSF} based on equations [2], [3] and [4], and $n_{i0} = 1.2 \times 10^7$ cm^{-3} at 300 K.

Table 2 gives the complete geometrical, material and performance parameters of the near optimum cell. Note that this optimized cell has a realistic expected efficiency of 22.61% and a V_{oc} of 901.6 mV. According to our model, higher V_{oc} values are obtainable at some sacrifice in J_{sc} and efficiency.

Because of heavy doping effects, our near-optimum design has relatively lighter dopings in the BSF and base. It may seem at first sight that with a BSF doping only ten times the base doping, the base/BSF interface would not be an effective reflector of minority carriers. However, higher BSF dopings result in the base/BSF interface being an even worse reflector of minority carriers because of heavy doping effects in the BSF.

Concluding Remarks

1. The primary factor limiting the V_{oc} in an n^+pp^+ solar cell is the heavy-doping factor in the p^+ BSF.

2. In a well-designed n^+pp^+ InP solar cell, the effective front SRV S_F has a significant effect on I_{sc} and η but a relatively minor effect on V_{oc}.

3. If the effective front SRV is reduced to $\sim 10^4$ cm/s and the HSR lifetime coefficients $\Gamma_{HSR,p}$, $\Gamma_{HSR,n}$ are increased by a factor of 10, then it is theoretically possible to obtain a V_{oc} of 902 mV and $\eta = 22.6\%$ at 1 AM0, 300 K, for an n^+pp^+ InP solar cell. Even higher V_{oc} values should be obtainable at a sacrifice in I_{sc} and η.

References

[1.] Russell E. Hart, NASA Lewis Research Center (LeRC), private communication.

[2.] Timothy J. Coutts, Solar Energy Research Institute (SERI), private communication.

[3.] C. Goradia, J.V. Geier, I. Weinberg, Solar Cells **25**, 235, 1988.

[4.] C. Goradia, J.V. Geier, I. Weinberg, *Conf. Rec. 19th IEEE Photovoltaic Specialists Conf.*, IEEE Publ. No. 87CH2400-0, 937, 1987,.

[5.] M.E. Klausmeier-Brown, P.D. DeMoulin, H.L. Chuang, M.S. Lundstrom and M.R Melloch, *Conf. Rec. 20th IEEE Photovoltaic Specialists Conf.*, IEEE Publ. No. 88CH2527-0, 503, 1988.

[6.] G. Augustine, A.W. Smith, A. Rohatgi, *Conf. Rec. 20th IEEE Photovoltaic Specialists Conf.*, IEEE Publ. No. 88CH2527-0, 903, 1988.

[7.] C.J. Keavney, M.B. Spitzer, Appl. Phys. Lett. **52**, 1439, 1988.

[8.] A.H. Yahia, T.J. Coutts, "Uncertainties in the Physical Parameters Used in Modelling InP Solar Cells: Part I, Effective Mass/Intrinsic Carrier Concentration", to be published.

Table 1

	Spire 6 Match (298 K)	Baseline Cell (300 K)
Grid Shadow	4.8%	4.0%
* Front SRV (cm/sec)	3.3×10^6	3.3×10^5
w_E, Å	400	200
$N_{D,\text{emitter}}$, cm^{-3}	1.0×10^{18}	5.0×10^{18}
* HD_E	1.4	0.632
* τ_{HSR}, ns	2	0.4
τ_{Rad}, ns	0.979	0.287
τ_p, ns	0.653	0.161
L_{pE}, μm	0.355	0.123
w_{base}, μm	3	2
$N_{A,\text{base}}$, cm^{-3}	2×10^{16}	2×10^{16}
* τ_{HSR}, ns	150	150
τ_{Rad}, ns	49.0	71.7
τ_n, ns	36.9	48.4
$L_{n,\text{base}}$, μm	19.4	22.4
w_{BSF}, μm	0.5	0.5
$N_{A,\text{BSF}}$, cm^{-3}	5×10^{18}	2×10^{18}
* HD_{BSF}	4.87	3.62
* τ_{HSR}, ns	0.6	1.5
τ_{Rad}, ns	0.196	0.717
τ_n, ns	0.143	0.477
$L_{n,\text{BSF}}$, μm	0.95	1.76
V_{oc}, mV	868	873
η	17.9%	19.23%

* Value obtained from Spire 6 match

Table 2

Best Theoretical Cell Design

Grid Shadow	4.0%
Front SRV	1×10^4 cm/sec
w_E	200 Å
$N_{D,\text{emitter}}$	3.0×10^{18} cm^{-3}
* $\text{HD}_E = \frac{n_{1E}}{n_{10}}$	0.837
* τ_{HSR}	6.667 ns
τ_{Rad}	0.478 ns
τ_p	0.431 ns
L_{pE}	0.227 μm
w_{base}	4 μm
$N_{A,\text{base}}$	8×10^{15} cm^{-3}
HD_{base}	1
* τ_{HSR}	3.75 μs
τ_{Rad}	179 ns
τ_n	171 ns
$L_{n,\text{base}}$	43.7 μm
w_{BSF}	250 μm
$N_{A,\text{BSF}}$	7.5×10^{16} cm^{-3}
HD_{BSF}	1
* τ_{HSR}	400 ns
τ_{Rad}	19.1 ns
τ_n	18.24 ns
$L_{n,\text{BSF}}$	12.57 μm

J_{sc}=39.94	mA/cm^2
V_{oc}=901.6	mV
J_{max}=38.59	mA/cm^2
V_{max}=804.4	mV
FF=86.21	%
η=22.61	%

Figure 1

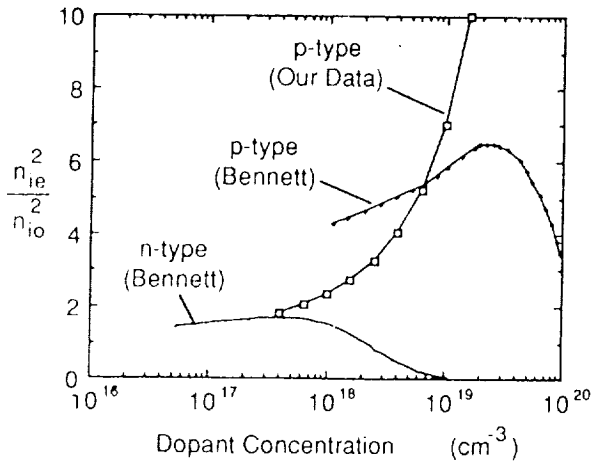

Effective intrinsic carrier concentration in n- and p-type GaAs.
Figure taken form M.E. Klausmeier-Brown et. al. Proc. of the 20th PVSC [5]

Figure 2

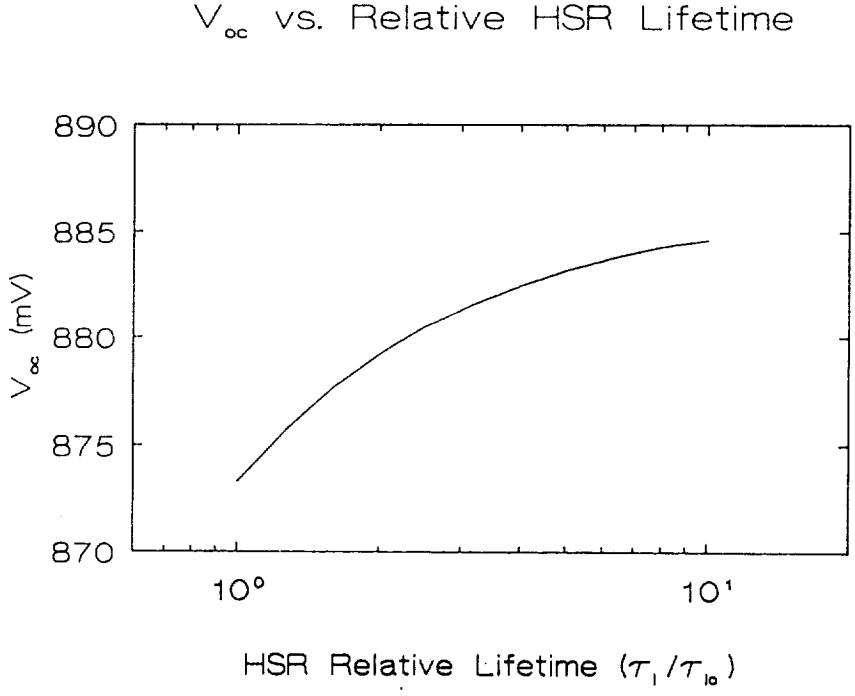

Figure 3

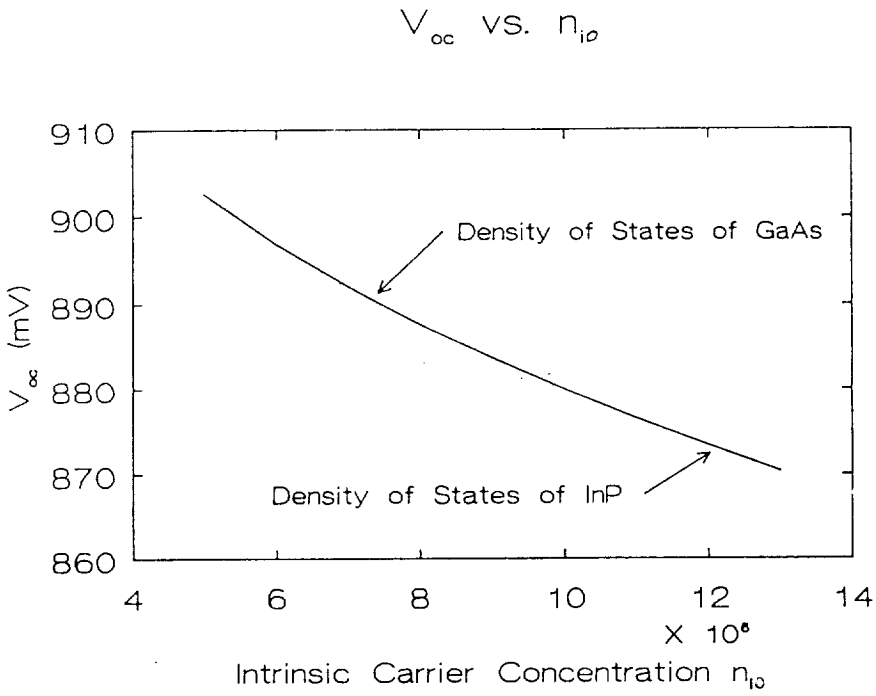

Figure 4

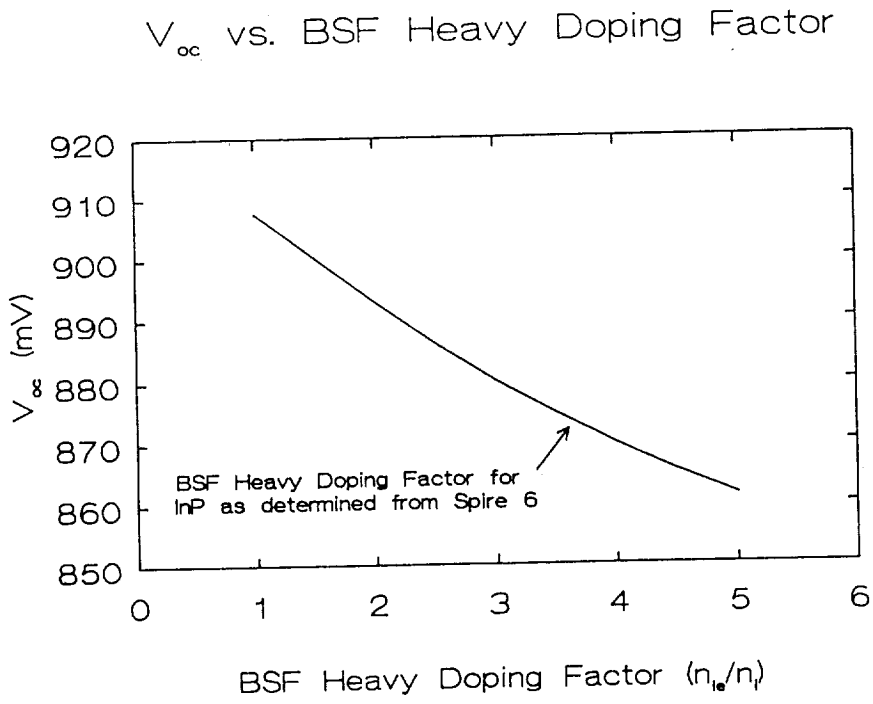

Figure 5

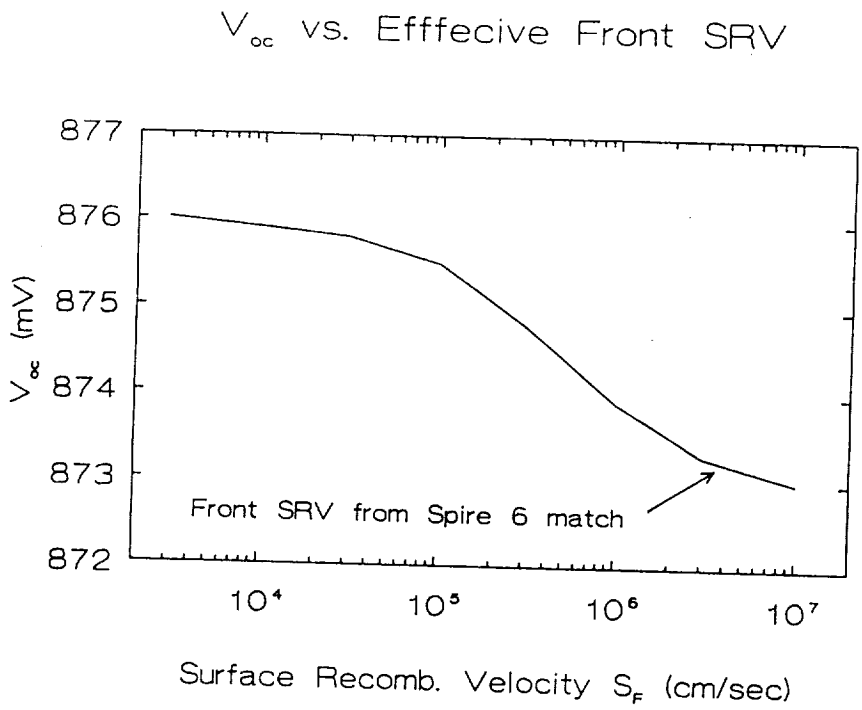
V_{oc} vs. Efffecive Front SRV
877
876
875
874
873
872
V_{oc} (mV)
Front SRV from Spire 6 match
10^4
10^5
10^6
10^7
Surface Recomb. Velocity S_F (cm/sec)